Inhibition of Carboxypeptidase A by D-Penicillamine: Mechanism and Implications for Drug Design†

Curtis R. Chong‡ and David S. Auld*

Center for Biochemical and Biophysical Sciences and Medicine and Department of Pathology, Harvard Medical School, Boston, Massachusetts 02115

Received January 19, 2000; Revised Manuscript Received April 6, 2000

ABSTRACT: Zinc metalloprotease inhibitors are usually designed to inactivate the enzyme by forming a stable ternary complex with the enzyme and active-site zinc. D-Cysteine inhibits carboxypeptidase, ZnCPD, by forming such a complex, with a K_i of 2.3 μM. In contrast, the antiarthritis drug D-penicillamine, D-PEN, which differs from D-Cys only by the presence of two methyl groups on the β-carbon, inhibits ZnCPD by promoting the release of the active-site zinc. We have given the name catalytic chelator to such inhibitors. Inhibition is a two-step process characterized by formation of a complex with the enzyme ($K_{i(initial)} = 1.2$ mM) followed by release of the active-site zinc at rates up to 420-fold faster than the spontaneous release. The initial rate of substrate hydrolysis at completion of the second step also depends on D-PEN concentration, reflecting formation of a thermodynamic equilibrium governed by the stability constants of chelator and apocarboxypeptidase for zinc ($K_{i(final)} = 0.25$ mM). The interaction of D-PEN and D-Cys with the active-site metal has been examined by replacing the active-site zinc by a chromophoric cobalt atom. Both inhibitors perturb the d−d transitions of CoCPD in the 500−600 nm region within milliseconds of mixing but only the CoCPD•D-Cys complex displays a strong S → Co(II) charge-transfer band at 340 nm indicative of a metal−sulfur bond. While the D-Cys complex is stable, the CoCPD•D-PEN complex breaks down to apoenzyme and Co(D-PEN)$_2$ with a half-life of 0.5 s. D-PEN is the first drug found to inhibit a metalloprotease by increasing the dissociation rate constant of the active-site metal. The ability of D-PEN to catalyze metal removal from carboxypeptidase A and other zinc proteases suggests a possible mechanism of action in arthritis and Wilson's disease and may also underlie complications associated with its clinical use.

The importance of zinc proteases in both normal and pathological processes makes them targets for drug design. The active-site zinc in these proteases is a particularly attractive target because the strength of a chelator−metal interaction increases the potency and specificity of an inhibitor. The success of such chelating inhibitors is demonstrated by the clinical efficacy of the ACE[1] inhibitor Captopril ([2*S*]-*N*-(3-mercapto-2-methylpropionyl)-L-proline) which has had a major impact on hypertension treatment (*1*).

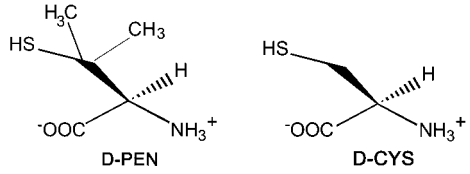

FIGURE 1: Structures of D-PEN and D-Cys.

Matrix metalloproteinases, MMP, are also appealing targets for drug design because of their involvement in cancer and arthritis, and several broad-spectrum chelating inhibitors are currently in phase I clinical trials (*2*).

The chelating agent D-penicillamine (D-PEN, Figure 1) has long been used to treat Wilson's disease, heavy metal poisoning, cystinuria, and rheumatoid arthritis. D-PEN (β,β-dimethylcysteine) is naturally produced by degradation of the thiazolidine ring after cleavage of the β-lactam ring in penicillin (*3*). L-Penicillamine (L-PEN) is not used clinically because of the high toxicity associated with its reaction with pyridoxal to form a thiazolidine ring, which leads to vitamin B6 deficiency (*3, 4*).

The metal-binding ability of D-PEN is believed to underlie its effectiveness in the treatment of Wilson's disease, an inherited disorder of copper metabolism. D-PEN is thought to decrease excess copper levels in Wilson's disease by reducing Cu(II) to Cu(I) (*5*). Reduction is accompanied by a change in preferred geometry from square planar to

† This research was supported by NIH Grant GM-53265 to D.S.A. and by grants from the Harvard College Undergraduate Research Program, the Dean's Summer Research Award, and the Head Tutor's fund in the Department of Biochemical Sciences, Harvard University, to C.R.C.

* To whom correspondence should be addressed: e-mail David_Auld@hms.harvard.edu fax 617-566-3137.

‡ Present address: Medical Scientist Training Program, Johns Hopkins University School of Medicine, Baltimore, MD 21205; e-mail: crchong@post.harvard.edu.

[1] Abbreviations: ACE, angiotensin converting enzyme; CABS-Sepharose, [*N*-(*ε*-aminocaproyl)-*p*-aminobenzyl]succinyl-Sepharose 4B; CoCPD, cobalt carboxypeptidase A; CPD, apocarboxypeptidase A.; Dns, dansyl [5-(dimethylamino)naphthalene-1-sulfonyl]; D-PEN, D-penicillamine; Ellman's reagent, 5,5′-dithiobis (2-nitrobenzoic acid); EDTA, ethylenediaminetetraacetic acid; Hepes, *N*-(2-hydroxyethyl)-piperazine-*N*′-2-ethanesulfonic acid; MAT, matrilysin, MMP, matrix metalloproteinases; OP, *o*- (1,10-) phenanthroline; PAR, 4-(2-pyridylazo)resorcinol; PEN, D- and L-penicillamine; TLN, thermolysin; ZnCPD, zinc carboxypeptidase A.

10.1021/bi000101+ CCC: $19.00
Published on Web 05/31/2000

tetrahedral and a change in net charge, both of which are less favorable for protein binding. Although EDTA binds copper with equal or greater affinity, it is thought to have a lower efficacy than D-PEN in the treatment of Wilson's disease due to its inability to reductively chelate copper.

D-PEN has also been used for 30 years to treat rheumatoid arthritis but its mechanism of action remains unknown (*3, 6*). Numerous double-blind clinical trials have established that D-PEN is as effective or more effective than other antiarthritis drugs (*6*). Unlike antiinflammatory agents, D-PEN slows progression of rheumatoid arthritis and is classified as a disease-modifying antirheumatic drug (*7*). D-PEN has been postulated to scavenge free radicals, modify collagen, and disrupt immune system proteins, but no general theory of its mechanism of action is widely accepted because none have been strongly supported by laboratory or clinical observations (*3*).

The current understanding of metalloprotease involvement in the pathogenesis of arthritis suggests that the efficacy of D-PEN may be explained by inhibition of zinc proteases involved in remodeling the extracellular matrix. Because D-PEN can chelate zinc with its thiol, amino, or carboxylate groups, we tested it for inhibition of three zinc proteases, matrilysin, thermolysin, and carboxypeptidase A, since these enzymes represent the matrix metalloprotease, metalloendoprotease, and metalloexoprotease families, respectively. To study the effects of stereochemistry and chemical structure on chelator potency and mechanism, L-PEN was examined along with the analogues D- and L-Cysteine, which differ from D- and L-PEN only by the absence of two methyl groups on the β-carbon (Figure 1). A preliminary report of this study has been made (*8*).

MATERIALS AND METHODS

Materials. Carboxypeptidase A (Cox), ZnCPD, and thermolysin, TLN, were obtained from Sigma. Prior to use ZnCPD was purified on a CABS-Sepharose affinity column and recrystallized as previously described (*9, 10*); TLN was purified by recrystallization (*11*). Cobalt carboxypeptidase (CoCPD) was prepared from crystalline ZnCPD by removing the active-site zinc with 1,10-phenanthroline (OP) and reconstituting the apoenzyme with $CoCl_2$ (*12*). Active matrilysin (MAT) was expressed in *Escherichia coli*, refolded, and purified by heparin−agarose chromatography as previously described (*13*). Enzyme concentrations were determined by absorbance, with ϵ_{280} of 64 500 M^{-1} cm^{-1} for ZnCPD (*14*), 61 500 M^{-1} cm^{-1} for TLN (*11*), and 33 000 M^{-1} cm^{-1} for MAT (*13*).

Synthetic fluorescent peptide substrates were synthesized, purified, and characterized as previously described (*15, 16*). Substrate concentration was determined by absorbance of the dansyl group, with $\epsilon_{340} = 4300$ M^{-1} cm^{-1}. Chemicals were reagent-grade and at least 99% pure. D-PEN and 4-(2-pyridylazo)resorcinol (PAR) were from Aldrich. L-PEN and D-PEN disulfide were from Fluka; D- and L-Cys, calcium, and Hepes buffer were from Sigma. All thiol inhibitors were prepared fresh each day. Experiments with Ellman's reagent, 5,5′-dithiobis(2-nitrobenzoic acid), showed disulfide formation did not occur over the time course of the experiments.

All experiments were performed under metal-free conditions. No metal contamination of inhibitors was found by using PAR. Buffers were extracted with dithizone (*17*). Dialysis tubing was rendered metal-free by heating in deionized water (*18*), and glassware was acid-washed in 1/3 HNO_3/deionized water.

Stopped-Flow Experiments. Kinetics were performed with an Applied Photophysics SX.18MV stopped-flow reaction analyzer. Solutions for stopped-flow experiments were extensively degassed to prevent artifacts from air bubbles. The fastest measurable half-life was found to be 0.6 ms by using the reduction of 2,6-dichorophenolindophenol by L-ascorbic acid as the test reaction (*19*). All reactions were performed at 25 ± 0.2 °C.

Substrate hydrolysis catalyzed by ZnCPD, 1×10^{-6} M, was measured in 1 M NaCl and 20 mM Hepes, pH 7.5, with the fluorescent substrate Dns-GGW. The substrate concentration, 1×10^{-5} M, was well below its reported K_m (*20*), ensuring a good steady-state approximation. MAT, 5×10^{-7} M, was assayed in 10 mM $CaCl_2$, 0.15 M NaCl, and 50 mM Hepes, pH 7.5, with Dns-PLALWAR, 2.5×10^{-6} M, well below its reported K_m (*13*). Dns-PLALWAR, 2.5×10^{-6} M, was also used to assay TLN, 1×10^{-7} M, in 10 mM $CaCl_2$, 0.1 M NaCl, and 50 mM Hepes, pH 7.5.

Initial velocity values were obtained by a linear plot of ≤10% of the substrate hydrolysis, monitored by following the increase in tryptophan fluorescence after excitation at 285 nm upon cleavage of the scissile bond. The change in fluorescence upon complete substrate hydrolysis was used to calculate micromoles of product produced. All substrate experiments were performed in the presence of a final concentration of 2.5% acetonitrile to ensure substrate solubility. Instantaneous, or rapid equilibrium, K_i values were determined by mixing inhibitor and substrate in one drive syringe of the stopped-flow instrument with enzyme in the other; at least 5 different inhibitor concentrations were used and at least three measurements of the initial rate were collected for each concentration. To determine K_i values, the reciprocal of the initial velocity, v, was plotted against inhibitor concentration according to eq 1. A single iteration was needed to determine the free inhibitor concentration for the inhibition of CPD A by D-Cys:

$$v = k_{cat}[S]/(K_m(1 + [I]/K_i) \qquad \text{for } [S] \ll K_m \qquad (1)$$

A stopped-flow assay was also used to characterize time-dependent inhibition. In this assay, inhibitor and enzyme are premixed and loaded in one syringe of the stopped-flow instrument, and the reaction is initiated by the addition of substrate from the second syringe. The present version of the SX.18MV instrument, lacking the sequential flow option, has a lag time of approximately 45 s between the start of the preincubation period and data collection. However, the subsequent delays between successive mixing are only 5 s, thus allowing characterization of the time-dependent decrease in initial rate. A final K_i can be calculated from the final constant velocity and eq 1. This new stopped-flow assay is a more convenient alternative to other assays that test for time-dependent inhibition through progress curve analysis (*21*).

PAR Experiments. The chromophoric chelator PAR was used to measure zinc dissociation from ZnCPD. PAR has a high affinity for zinc with an apparent binding constant log $\beta_2 = 12.3$ ($K_1' = 4.0 \times 10^6$ M^{-1}, $K_2' = 5.5 \times 10^5$ M^{-1}) (*22,*

Table 1: Instantaneous K_i Values[a]

	K_i (mM)		
inhibitor	ZnCPD	TLN	MAT
D-Cys	0.0023 ± 0.0016	0.040 ± 0.0068	0.75 ± 0.13
L-Cys	0.35 ± 0.050	1.8 ± 0.25	1.6 ± 0.86
D-PEN	1.2 ± 0.18	1.9 ± 0.24	0.6 0 ± 0.22
L-PEN	1.7 ± 0.44	5.2 ± 1.4	0.42 ± 0.11
D-PEN disulfide	>27	>25	>45

[a] Conditions of assay are given in the Materials and Methods section. Error in K_i values was calculated from standard errors of the slope and *y*-intercept of Dixon plots.

23). Data were collected at 500 nm with a PAR concentration of 1.8 mM and the 0.2 mm path length of the stopped-flow reaction cell. The transmittance was set to 100% with buffer solution. The extinction coefficient at 500 nm was 61 500 M^{-1} cm^{-1} for the $Zn(PAR)_2$ complex. Enzyme was mixed in the stopped-flow instrument with PAR alone or with inhibitor to measure the rate of zinc dissociation. For preincubation experiments, PAR and inhibitor were mixed in the stopped-flow instrument with a preincubated solution of enzyme and inhibitor, so that the inhibitor concentration was constant throughout the reaction. The rate constant for the formation of the $Zn(PAR)_2$ complex was calculated from the absorbance change by use of the single-exponential fit program of the SX.18MV stopped-flow software package.

Rapid-Scanning Cobalt Experiments. The binding processes of D-Cys and D-PEN were studied spectroscopically with CoCPD. Electronic absorption spectra (50−800 scans) were obtained in the stopped-flow instrument over the region of 300−700 nm and time range of 1.3 ms−120 s. All reactions were performed at 25 ± 0.2 °C, and a buffer of 1 M NaCl and 20 mM Hepes, pH 7.5, was used. Spectra were normalized in the 680−700 nm region to remove noise due to lamp drift during longer runs. Rate constants were determined by use of the Pro K global analysis software suite.

RESULTS

Inhibition Studies. Instantaneous K_i values show that the stereochemistry and chemical structure of chelating ligands are important determinants of potency (Table 1). This effect is most apparent for ZnCPD: D-Cys inhibits ZnCPD with a K_i of 2.3 μM while its enantiomer L-Cys inhibits with a K_i 150-fold higher (K_i = 0.35 mM). The K_i for D-PEN, which differs from D-Cys only by the presence of two methyl groups on the β-carbon, is 520 times higher (1.2 mM). A similar pattern of inhibition is observed for TLN: D-Cys inhibits TLN with a K_i of 40 μM and is approximately 45 times more potent than D-PEN and L-Cys. Inhibition of MAT by D- and L-PEN is slightly greater than inhibition of ZnCPD and TLN, while D-Cys is a much more potent inhibitor of ZnCPD and TLN. D-PEN disulfide does not inhibit any of the enzymes tested, suggesting that the thiol group is essential for inhibition.

When D-PEN and ZnCPD are preincubated, the initial velocity of substrate hydrolysis decreases exponentially with time and becomes constant within 200 s (Figure 2). As the D-PEN concentration is raised, the final velocity decreases. This dependence on D-PEN concentration gives a final K_i value, 0.25 mM, that is 5 times lower than the initial K_i. The first-order rate constant, *k*, for this time-dependent

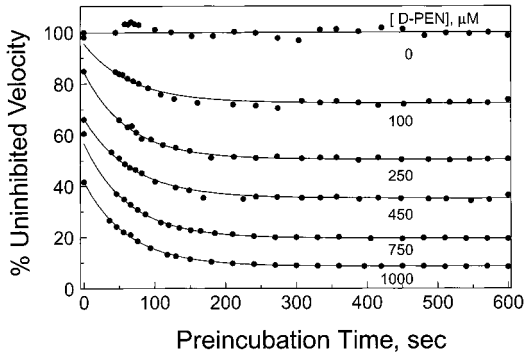

FIGURE 2: Exponential time-dependent inhibition of ZnCPD by D-PEN. Each point (●) represents an initial velocity, obtained at 5 s intervals in the stopped-flow instrument expressed as a percentage of the initial uninhibited velocity. The solid lines are obtained from eq 2. For clarity, data for D-PEN concentrations of 0.35, 0.55, and 3.3 mM are not included.

ZnCPD inhibition is determined from

$$v_t = (v_i - v_f)\, e^{-kt} + v_f \qquad (2)$$

where v_i is the initial velocity at time zero, v_f is the initial velocity after equilibration of enzyme and inhibitor, and v_t is the velocity at any time *t*. The rate constants for the time-dependent inhibition of ZnCPD are independent of D-PEN concentration, averaging 0.0157 ± 0.003 s^{-1}. Time-dependent inhibition of ZnCPD is also seen with L-PEN but not L-Cys or D-Cys.

The time-dependent inhibition of ZnCPD observed by D- and L-PEN is indicative of a two-step mechanism. Two mechanisms could explain this time-dependent inhibition. In one such mechanism, penicillamine could act as a slow-binding inhibitor where the instantaneous K_i represents the formation of a weakly bound EI complex and the final K_i* is due to isomerization to a more stable EI* complex (*21*):

Mechanism 1

$$EZn + I \rightleftharpoons I{\cdot}EZn \rightleftharpoons {*}I{\cdot}EZn$$

Slow-binding inhibitors of zinc proteases are well characterized for TLN, ACE, and aminopeptidases. The antihypertensive drug Captopril acts as a slow-binding inhibitor of ACE, and the natural products amastatin and bestatin inhibit aminopeptidases by a slow-binding mechanism (*21*).

A second mechanism that could explain time-dependent inhibition is the removal of zinc. In this scenario, the instantaneous K_i is due to a formation of a complex between D-PEN and the enzyme. The final inhibition constant, $K_{i(final)}$, reflects the formation of a thermodynamic equilibrium between apoenzyme and inhibitor that is governed by the stability constants of these two chelators for zinc (mechanism 2). In this mechanism the inhibitor could bind and release either zinc or the ZnI complex if it binds directly to the metal in the first step.

Mechanism 2

$$EZn + I \rightleftharpoons I{\cdot}EZn \rightleftharpoons I{\cdot}E + Zn$$

$$Zn + I \rightleftharpoons Zn(I)_2$$

Mechanisms 1 and 2 differ in the location of the active-site zinc during the final step. In mechanism 1, enzyme is bound

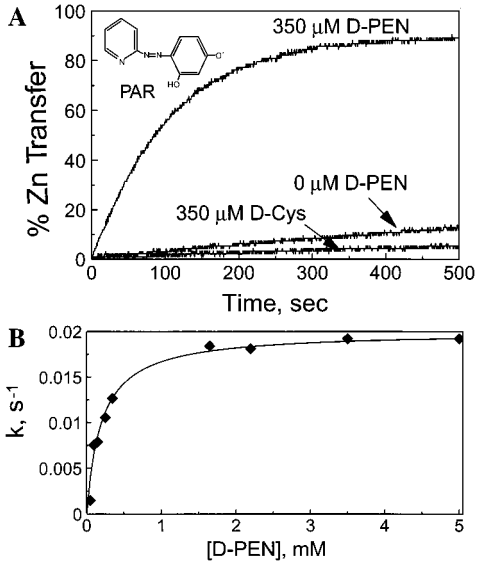

FIGURE 3: (A) Comparison of zinc transfer from ZnCPD, 5 μM, to PAR, 1.8 mM, alone or in the presence of 0.35 mM D-PEN or 0.35 mM D-Cys (all concentrations after mixing). Zinc transfer to PAR is monitored by the increase in absorbance at 500 nm. (B) Concentration dependence of the rate constant for the D-PEN-catalyzed transfer of zinc from ZnCPD to PAR when the enzyme, 10 μM, is mixed with 3.6 mM PAR and increasing concentrations of D-PEN. The solid line is derived from the function $k_s = 0.020$ s^{-1}[D-PEN]/(0.2 mM + [D-PEN]).

to both zinc and inhibitor in the final step, but in mechanism 2, some zinc dissociates and is bound by inhibitor.

Detection of Zn Release by Use of PAR. The location of zinc in the final step can be used to differentiate between mechanisms 1 and 2. The absorption maximum for the chelator PAR changes from 412 to 500 nm upon binding Zn (*22*). The $Zn(PAR)_2$ complex forms within 2 ms after mixing 10 μM $ZnCl_2$ with 3.6 mM PAR (data not shown).

When 3.6 mM PAR is mixed with 10 μM ZnCPD, zinc dissociates very slowly in a first-order process with a rate constant of 4.8×10^{-5} s^{-1} or a half-life of 14 400 s (Figure 3A). Zinc dissociation is slower when enzyme is mixed with PAR in the presence of 0.35 mM D-Cys, suggesting that D-Cys protects the active-site zinc from removal. At D-Cys concentrations as high as 5 mM, essentially no zinc dissociation is observed. In marked contrast, when enzyme and PAR are mixed in the presence of 0.35 mM D-PEN the first-order rate constant for zinc dissociation ($k = 1.3 \times 10^{-2}$ s^{-1}; half-life of 53 s) is 264 times that of the spontaneous dissociation rate constant and 92% of the zinc is transferred to PAR in 300 s (Figure 3).

The first-order rate constant for zinc dissociation shows a hyperbolic relationship to D- and L-PEN concentrations (Figure 3B). It reaches a maximum of 0.020 s^{-1} at a D-PEN concentration of 5 mM, representing a 420-fold increase over the rate constant for spontaneous dissociation of zinc from ZnCPD. This rate constant is close to the average rate constant for the decrease in enzyme activity observed when D-PEN is preincubated with ZnCPD and mixed with substrate (0.020 s^{-1} versus 0.016 s^{-1}). The maximum rate constant of zinc dissociation in the presence of L-PEN (0.018 s^{-1}) is nearly identical.

As PEN concentrations increase, the amount of zinc transferred from the enzyme to PAR decreases progressively. This decrease is also observed when 5 μM $ZnCl_2$ is preincubated with increasing D-PEN concentrations and a constant concentration of 1.8 mM PAR, indicating that D-PEN effectively competes with PAR for zinc (data not shown).

The PAR results suggest that D-PEN can mediate zinc transfer either by making the enzyme-bound zinc more accessible to PAR or by catalyzing its release. To differentiate between these two possibilities, we preincubated D-PEN and ZnCPD prior to the addition of PAR. If D-PEN labilizes the active-site zinc for PAR removal, then the rate constant for zinc transfer should be the same as the rate constant observed without preincubation (Figure 3A). If D-PEN removes metal during the preincubation period, the rate constant for zinc transfer from ZnCPD to PAR should equal the rate constant for zinc transfer between the $Zn(D\text{-}PEN)_2$ complex and $Zn(PAR)_2$.

A preincubation time of 200 s is initially chosen since the second step in the inhibition experiments is nearly complete within this time (Figure 2). D-PEN at a concentration of 1.5 mM is preincubated with 10 μM ZnCPD for 200 s and then mixed with 3.6 mM PAR and 1.5 mM D-PEN in the stopped-flow instrument. Under these conditions two phases of zinc transfer to PAR are observed: the first two seconds of the reaction after PAR addition is termed the "fast phase," and the remaining time up to 500 s is referred to as the "slow phase"(Figure 4).

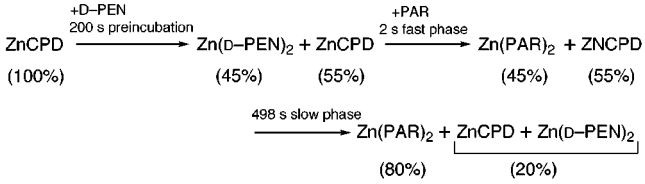

Under these conditions, 45% of the zinc is transferred to PAR in the fast phase with a first-order rate constant of 5.6 s^{-1}. The same rate constant is obtained when a solution of 10 μM $ZnCl_2$ and 1.5 mM D-PEN is mixed with 1.5 mM D-PEN and 3.6 mM PAR, indicating D-PEN releases zinc from the enzyme during the preincubation period. In the next 498 s slow phase, 64% of the remaining zinc is transferred to PAR. By 500 s, at least 80% of the zinc is transferred from ZnCPD to PAR, an amount similar to that observed with no preincubation. Full zinc transfer to PAR does not occur because both D-PEN and apoenzyme compete with PAR for binding zinc (see above). The addition of PAR after preincubation of ZnCPD and D-PEN for 1000 s does not change the rate constant or extent of zinc transfer, suggesting the equilibrium between D-PEN and enzyme is complete within 200 s. The fast phase does not occur if D-PEN, ZnCPD, and PAR are mixed simultaneously (Figure 4).

The rate constants for zinc transfer in the fast phase for eight D-PEN concentrations are identical to the rate constants when the same concentrations of D-PEN are preincubated with $ZnCl_2$ and then mixed with D-PEN and PAR (Figure 5A). As D-PEN concentration increases, the rate constant for zinc transfer to PAR decreases, likely due to change in the rate-determining steps involving formation of mono-Zn·D-PEN and/or mono-Zn·PAR complexes. Thus D-PEN removes zinc rapidly from ZnCPD over the concentration range of 0.25−5 mM. As the preincubated D-PEN concentration increases, more zinc is transferred to PAR in the fast phase,

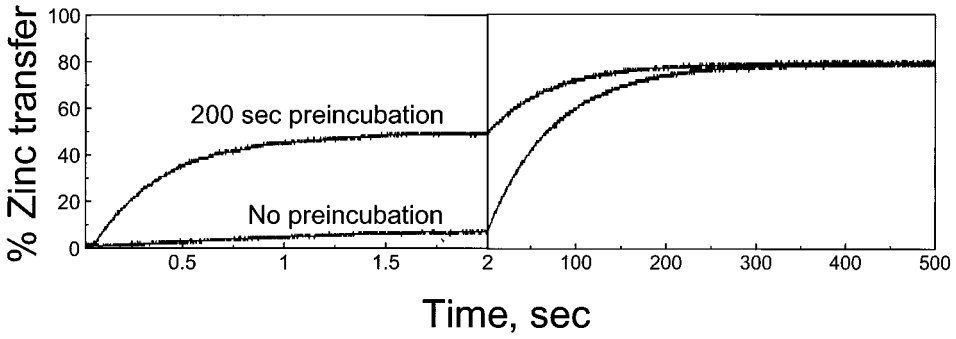

FIGURE 4: D-PEN, 1.5 mM, and ZnCPD, 10 μM, are preincubated for 200 s and mixed with 3.6 mM PAR and 1.5 mM D-PEN in the stopped-flow instrument. The first two seconds after mixing is termed "fast phase"; the remaining 498 s of the reaction is called the "slow phase."

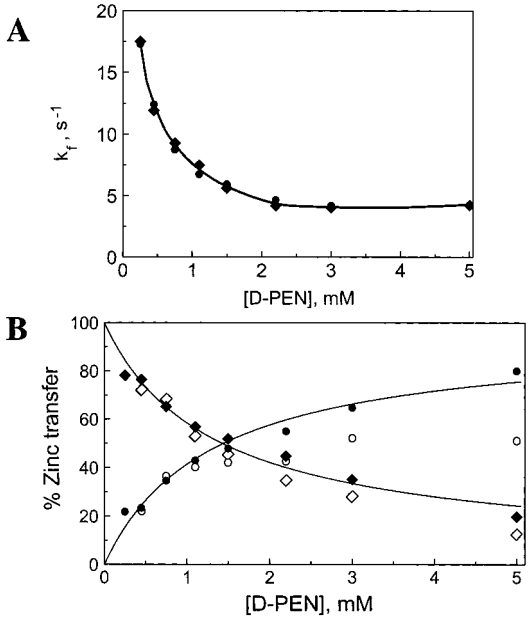

FIGURE 5: ZnCPD, 10 μM, is preincubated with increasing concentrations of D-PEN for 200 s and mixed with 3.6 mM PAR and D-PEN in the stopped-flow instrument and the (A) rate constant of fast phase and (B) amplitudes of the fast and slow phase of the reaction are measured. (A) The "fast phase" rate constant of zinc transfer to PAR, k_f (◆), is identical to the rate constant of transfer when 10 μM $ZnCl_2$ (●) is preincubated with D-PEN and mixed with 3.6 mM PAR and D-PEN. (B) The extinction coefficient of the $Zn(PAR)_2$ complex is used to determine the effect of D-PEN concentration on the extent of zinc transfer in the fast (○) and slow (◇) phases. Corrected amplitude values for the fast (●) and slow (◆) phases are calculated on the basis of the assumption that the average 99.7% total Zn transfer observed for the lowest three D-PEN concentrations should be the same for the higher concentrations. The theoretical curve for the amplitude values in the fast phase is obtained from the function $Amp_f = 95\%([D\text{-PEN}]/(1.3\text{ mM} + [D\text{-PEN}])$. The theoretical curve for the slow-phase amplitudes is obtained by subtracting these values from 99.7%.

while the amount transferred during the slow phase decreases (Figure 5B). The extent of zinc transfer detected in the fast phase shows a hyperbolic relationship to the D-PEN concentration. This result is expected since the free enzyme is progressively converted into the ZnCPD•D-PEN complex as the D-PEN concentration increases. This species in turn dissociates to apoenzyme and Zn or Zn(D-PEN), which is rapidly converted to $Zn(D\text{-PEN})_2$. Since the zinc concentration is fixed, more metal removal in the fast phase results in less metal removal in the slow phase.

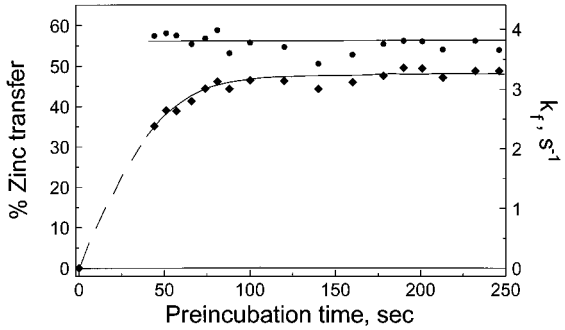

FIGURE 6: Dependence of the extent of zinc removal by D-PEN as measured by PAR in fast phase (◆) and rate constant, k_f (●), on preincubation time. D-PEN, 1.5 mM, and ZnCPD, 10 μM, are preincubated and mixed with PAR, 3.6 mM, and D-PEN, 1.5 mM, at 5−7 s intervals.

The extent of zinc transfer in the fast phase over time is measured by decreasing the preincubation time. D-PEN, 1.5 mM, and ZnCPD, 10 μM, are preincubated and mixed with PAR, 3.6 mM, and D-PEN,1.5 mM, in the stopped-flow instrument. The reaction is initiated after 44 s of preincubation due to a lag time for the present configuration of the stopped-flow instrument. At time intervals of 5−7 s, the preincubated D-PEN and ZnCPD solution is mixed with PAR, and conversion of $Zn(D\text{-PEN})_2$ into $Zn(PAR)_2$ is followed by the increase in absorbance at 500 nm in the fast phase. The amplitudes and first-order rate constants of zinc transfer for the fast phase are plotted in Figure 6. As preincubation time increases, more zinc is transferred to PAR in the fast phase, reflecting the increased conversion of enzyme-bound zinc to $Zn(D\text{-PEN})_2$ during the preincubation period. The rate constant for zinc transfer is the same regardless of preincubation time because it is related only to the kinetic parameters for the association and dissociation of zinc with D-PEN and PAR. After about 200 s, the amount of zinc removed from the enzyme remains constant at 50%, representing a thermodynamic equilibrium governed by the affinities of D-PEN and apoenzyme for zinc. The time necessary to reach this equilibrium is in agreement with experiments where time-dependent inhibition is observed by preincubating D-PEN and ZnCPD and adding substrate to monitor the reaction (Figure 2). A constant velocity is reached in the substrate hydrolysis experiments after 200 s of preincubation, which corresponds to the time necessary to reach equilibrium between D-PEN, CPD, and PAR with zinc. This suggests that the time-dependent decrease in enzyme velocity seen in Figure 2 is due to D-PEN-catalyzed zinc removal.

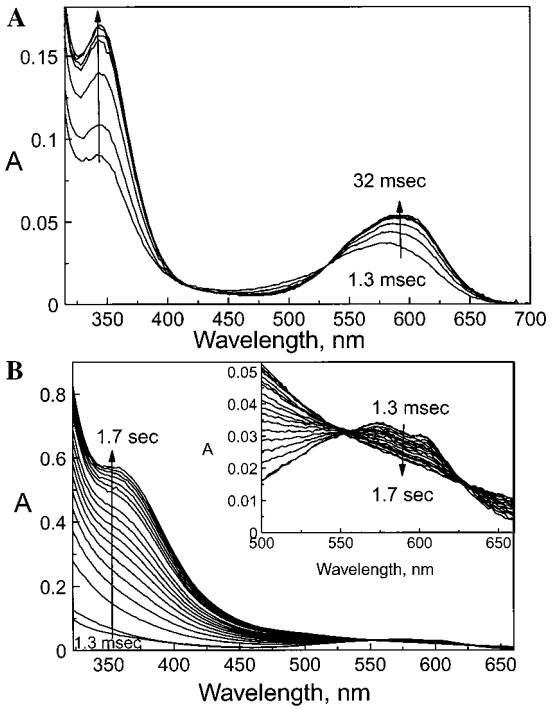

FIGURE 7: (A) Visible absorption spectra of the formation of CoCPD·D-Cys complex upon mixing D-Cys, 0.8 mM, and CoCPD, 0.33 mM, in the stopped-flow instrument and scanning at 1.28, 3.84, 6.4, 8.96, 11.2, 14.08, 21.6, and 32 ms. The spectral changes occur with half-life of 3.85 ms. (B) Visible absorption spectra of the breakdown of CoCPD·D-PEN complex after mixing D-PEN, 40 mM, and CoCPD, 0.33 mM, in the stopped-flow instrument and scanning at 1.28, 26.8, 78.1, 154.9, 231.7, 308.5, 385.3, 462.1, 538.9, 641.3, 743.7, 846.1, 948.5, 1050.8, 1178.9, 1306.9, 1438.9, 1562.9, and 1716.5 ms. The spectral change has a half-life of 0.5 s. Inset: Expanded absorbance changes in the 500−650 nm region.

When L-PEN and ZnCPD are preincubated for 200 s, zinc transfer in the "fast" and "slow" phases is similar to that observed for D-PEN and ZnCPD, indicating that the enantiomers share a similar mechanism. No metal transfer is observed with D-Cys and ZnCPD for preincubation times up to 1000 s or for D-Cys concentrations up to 5 mM.

Cobalt CPD Spectroscopy. Although the PAR and substrate experiments suggest D-PEN inhibits ZnCPD and CoCPD by forming a complex with the enzyme followed by release of the active-site metal, direct evidence requires detection of the intermediate. Substitution of the paramagnetic cobalt ion for the active-site zinc permits study of the coordination geometry and functional properties of the enzyme (*24*−*26*). Binding of a thiolate ligand to the active-site cobalt perturbs the d → d transition and charge-transfer regions of the CoCPD spectrum (*27*). Thus rapid-scanning spectral studies of CoCPD can be used to detect formation of a complex between D-PEN or D-Cys, with CoCPD or free cobalt ions.

D-Cys, 0.8 mM, and CoCPD, 0.334 mM, at pH 7.5 are mixed in the stopped-flow instrument and the spectral changes from 300 to 700 nm are obtained every 2.6 ms. Under these conditions the enzyme should be saturated with inhibitor, based on the K_i of D-Cys for CoCPD of 22 μM. The spectral changes that occur upon mixing CoCPD and D-Cys are complete within 32 ms (Figure 7A). The absorbance increases in two regions, one centered at 350 nm and the other at 590 nm (Figure 7A). This increase is a rapid process, with a first-order rate constant of 180 s^{-1} (half-life of 3.85 ms).

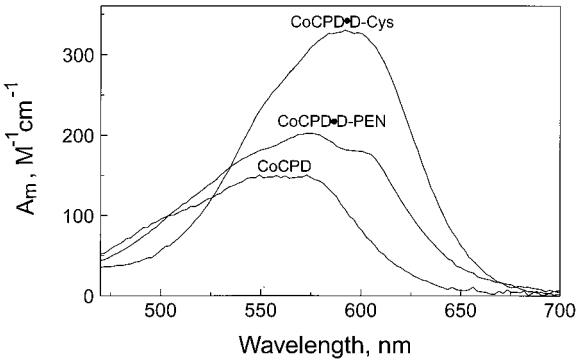

FIGURE 8: Comparison of the spectra of CoCPD and its D-PEN and D-Cys complexes. Conditions were as given in the Figure 7 caption. For the CoCPD·D-Cys complex the spectrum is the average of the 29.4, 32, and 34.56 ms scans while for the D-PEN intermediate the 1.28, 3.84, and 6.4 ms scans are averaged.

The absorption spectrum of CoCPD between 340 and 650 nm at pH 7.5 has a broad shoulder near 500 nm and maxima at 550 and 573 nm (Figure 8) in close agreement with earlier studies (*24*). The CoCPD·D-Cys complex displays a broad maximum at 592 nm with an ϵ of 330 cm^{-1} M^{-1} and a shoulder near 550 nm with an ϵ of about 235 cm^{-1} M^{-1}. This spectrum is quite similar to that observed for the ternary CoCPD·L-Phe·N_3^- complex in which the azide is a ligand to the cobalt (*28*), suggesting the sulfhydryl group of D-Cys may be a ligand in the CoCPD·D-Cys complex.

A new transition that is not present in the absorption spectrum of CoCPD is observed with a λ_{max} at approximately 346 nm (ϵ = 1018 M^{-1} cm^{-1}) (Figure 7A). This increase of absorbance in the 300−350 nm region is significant because this is the region of the S → Co(II) charge-transfer band (*27*). The observed extinction coefficient is consistent with that reported for mercaptan inhibitors of carboxypeptidase and thermolysin that bind the active-site cobalt with one S → Co(II) bond ($\epsilon \approx$ 900 M^{-1} cm^{-1}) (*24*, *27*). Since the final spectrum is distinct from the spectrum observed when D-Cys is mixed with Co(II) (ϵ_{343} = 5200 M^{-1} cm^{-1}), D-Cys does not remove cobalt from the enzyme. Hence D-Cys inhibits CoCPD by forming a stable ternary complex with the active-site cobalt.

The effect of D-PEN on the absorption spectrum of CoCPD, 0.167 mM, is examined over the D-PEN concentration range of 0.4−50 mM. Data from experiments in which 20 mM D-PEN is used are presented here as representative spectra (Figure 7B) since the instantaneous K_i of D-PEN on CoCPD catalysis is 9 mM. At this D-PEN concentration all spectral changes are essentially complete within 1.7 s after mixing. Two pronounced spectral changes occur over two different time ranges. By the first scan, taken at 1.3 ms, the spectrum in the 500−650 nm region is distinct from that of CoCPD alone, indicative of a very rapid ($k \geq$ 1000 s^{-1}) binding of D-PEN to form an E·I complex with a perturbed Co(II) coordination sphere. The CoCPD·D-PEN complex displays a distinct maximum at 574 nm (ϵ = 202 M^{-1} cm^{-1}) and two others near 549 and 605 nm with ϵ = 181 M^{-1} cm^{-1} and ϵ = 202 M^{-1} cm^{-1} (Figure 8). Importantly, no distinct S → Co(II) charge-transfer band in the 350 nm region is observed in the first spectrum. Hence the intermediate does not involve a bond between the cobalt atom and the thiol of

D-PEN. The spectrum of the intermediate D-PEN complex is similar to that seen for the CoCPD·D-Phe complex which has absorption bands at 545, 580, and 602 nm with extinction coefficients of 165, 205, and 180 M^{-1} cm^{-1}, respectively, at pH 7.1 (*24*).

By 1.7 s the distinct absorbance in the 500−650 nm region is gone (Figure 7B, inset). This decrease in absorbance is in marked contrast to the unchanging spectrum of the D-Cys complex after the first 30 ms (Figure 7A) and supports the hypothesis that D-PEN removes metal from CoCPD whereas D-Cys forms a ternary complex. The absorbance decrease in the 500−650 nm region for D-PEN is concomitant with an increase in absorbance centered around λ_{max} at 355 nm (ϵ = 3446 M^{-1} cm^{-1}) indicative of formation of sulfur−cobalt bonds. The time-dependent absorption changes follow first-order kinetics with a rate constant of 1.3 s^{-1} (half-life of 0.5 s). The absorption spectra between 1.7 and 8 s (15 half-lives) are essentially the same (data not shown). The final spectrum has properties (maximum near 350 nm, ϵ = 3446 M^{-1} cm^{-1}) quite similar to that of the S → Co(II) charge-transfer band properties of the complex formed between D-PEN and $CoCl_2$ (λ_{max} at 348 nm, ϵ = 4125 M^{-1} cm^{-1}). These data indicate D-PEN promotes release of cobalt from CoCPD via an intermediate that perturbs the environment around the active-site metal. Experiments with PAR present also demonstrate that D-PEN assists cobalt transfer from CoCPD to PAR (data not shown).

DISCUSSION

Penicillamine and cysteine have been reported to be inhibitors of carboxypeptidase A but their mechanisms of inhibition have never been characterized. Carboxypeptidase A is completely inhibited by 10 mM D,L-cysteine (*29*), and a study on the proteolysis of bradykinin in rheumatoid arthritis shows carboxypeptidase B to be completely inhibited by 0.13 mM D,L-PEN in a 3-h progress-curve assay (*30*). Both reports used only one concentration of Cys or PEN and no mechanistic work was performed. The effects of stereochemistry were not studied because racemic mixtures of inhibitor were used. Our studies on inhibition by the cysteine/penicillamine family of sulfhydryl-containing amino acids indicate inhibition of ZnCPD by two markedly different mechanisms. D-PEN promotes the removal of zinc from the enzyme, whereas D-Cys prevents zinc removal by forming a stable ternary complex.

Three mechanisms describing the action of chelating inhibitors are summarized in Figure 9. Inhibition of enzymatic activity can be due to formation of a stable ternary complex or can arise from metal removal by an S_N1- or S_N2-type mechanism (*31, 32*). Thus some chelating inhibitors such as D-Cys form a stable, ternary enzyme·metal·inhibitor complex (mechanism I in Figure 9). Other compounds such as EDTA and thionein scavenge metal that spontaneously dissociates from the enzyme by an S_N1 mechanism (mechanism II in Figure 9). D-PEN inhibits ZnCPD by first binding to the enzyme and then promoting release of the active-site zinc through an S_N2-type mechanism (mechanism III in Figure 9). We have given the name catalytic chelator to such inhibitors since they increase the dissociation rate constant for release of the metal and then act as recipients for the free metal. They could do this through a number of different

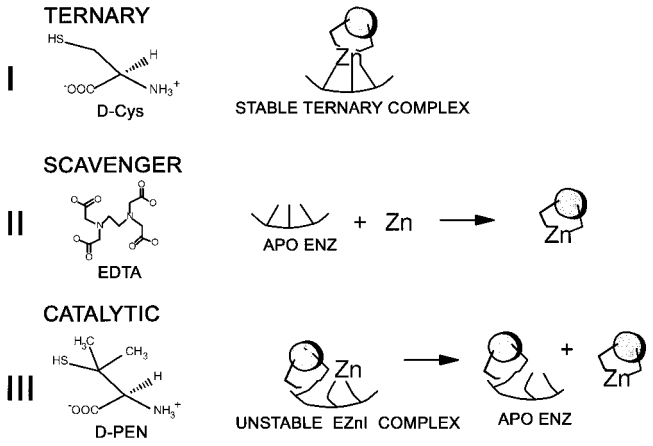

FIGURE 9: Schematic of three mechanisms of metalloprotease inhibition. D-Cys, D-PEN, and EDTA are given as representative inhibitors for such mechanisms. In the case of the catalytic chelator mechanism, the inhibitor may not bind to the apoenzyme if it forms an unstable ternary complex.

pathways. They might disrupt the scaffolding of the metal complex and cause the metal to dissociate faster either by itself or through the action of a second chelator molecule. Alternatively they could bind to the metal through one of their liganding atoms and to other regions of the active center, thus destabilizing metal binding and leading to dissociation of a metal−chelator complex. An unstable ternary complex formed between cobalt carbonic anhydrase and 2,6-pyridinedicarboxylate has been observed by cobalt absorption spectroscopy (*33, 34*). In addition, pH-indicator studies of the interaction of 1,10-phenanthroline and cobalt carboxypeptidase yield saturation kinetics indicative of an unstable intermediate (*35*).

Our results extend the observation that the stereochemistry and chemical structure of a chelating ligand contribute to the potency of inhibitors that act according to mechanism I in Figure 9. D-Cys is an 85-fold more potent inhibitor of ZnCPD than its L-enantiomer. Thiol chelators with D stereochemistry have also been reported to be more potent inhibitors of ACE and of human neutrophil and fibroblast collagenases (*1, 36*).

Cobalt spectroscopy establishes that D-Cys binds the active-site metal with its thiol side chain (Figure 8). This might be considered surprising since binding of anions to the active-site metal of carboxypeptidase is usually precluded by the interaction of the metal-bound water molecule and carboxylate of Glu-270 (*37*). However, anions do bind to the active-site metal in the L-Phe and D-Phe enzyme complexes because the protonated α-amino group of the inhibitor is postulated to disrupt the interaction of the Glu-270 carboxylate/zinc-bound water (*10, 28, 38, 39*). No X-ray crystallographic studies have been performed with the L-Phe complex, but results with the D-Phe complex demonstrate the existence of the postulated salt bridge between the carboxylate of Glu-270 and the amino group of D-Phe (*40*). In addition, the D-Phe carboxylate interacts with Arg-145, and the phenyl ring binds in the hydrophobic substrate pocket. Since the water is no longer H-bonded to the Glu-270 carboxylate, it can be displaced by anions. D-Cys could likely displace the water by forming such a complex and use its sulfhydryl group as the equivalent of an anionic ligand.

The traditional approach to drug design varies the chemical structure of a chelating ligand to improve inhibitors that mimic the substrate or an intermediate of the metalloenzyme catalysis. Compounds that form tight ternary complexes with low K_i values are used as templates to design inhibitors that bind with even greater affinity. This methodology was used in the design of chelators that inhibit ACE (*1*) and is currently in use to develop better MMP inhibitors (*41*−*44*). The assumption underlying this approach is that *all* inhibitors act according to mechanism I in Figure 9.

Our results demonstrate, however, that the chemical structure of a chelating ligand can change the mechanism of inhibition. The addition of two methyl groups to the β-carbon of D-Cys changes the inhibition mechanism from formation of a tight ternary complex (mechanism I in Figure 9) to catalytic removal of the active-site zinc (mechanism III in Figure 9).

The spectroscopic differences between D-Cys and D-PEN binding to CoCPD give insight on how these two methyl groups change the mechanism of inhibition. With D-Cys, an S → Co(II) charge-transfer band begins to appear immediately after mixing, indicating a bond forms between the inhibitor and active-site metal (Figure 7A). No such bond is observed in the D-PEN intermediate; the S → Co(II) charge transfer band only appears as the absorbance in the 500−650 nm region decreases, giving isobestic transitions at 550 and 630 nm (Figure 7B, inset). Thus, the bond between cobalt and the thiol of D-PEN forms after metal is removed from the enzyme. While the sulfur of D-PEN does not bind directly to cobalt when complexed to the enzyme, the spectrum of this intermediate closely resembles the spectrum of the CoCPD•D-Phe complex (*24*). Loss of the hydrogen bond between Glu-270 and the zinc-bound water causes the zinc to shift 1 Å away from Glu-270 toward Arg-127 (*40*). By acting as a secondary zinc ligand, Glu-270 likely increases the binding affinity of the enzyme for zinc. If D-PEN induces a similar change in the active site, loss of this interaction could increase the rate of zinc dissociation. In addition, D-PEN might weaken or disrupt other scaffolding interactions such as the one between Asp-143 and His-196. Indeed, disruption of scaffolding ligand interactions is known to decrease the affinity of enzymes for zinc (*45*−*47*).

The difference in chelator mechanisms observed for D-PEN and D-Cys complicates interpretation of inhibitor potency. Although the initial K_i for D-PEN is higher than that of D-Cys, D-PEN rapidly and completely inactivates ZnCPD in the presence of a secondary chelator with greater zinc affinity than D-PEN or CPD (Chong and Auld, manuscript in preparation). When D-PEN and ZnCPD are mixed with thionein or EDTA, the enzymatic activity of ZnCPD is eliminated within 20 min. Thionein or EDTA alone inhibits ZnCPD by chelating zinc that spontaneously dissociates from the enzyme (mechanism II in Figure 9). D-PEN accelerates zinc equilibration between ZnCPD and EDTA or thionein. Consequentially, the in vivo potency of D-PEN as a zinc enzyme inhibitor can be augmented by coadministration of secondary chelators such as EDTA or through the presence of natural chelators such as thionein or other metal-binding species. From a physiological perspective, such a mechanism of inhibition is essentially irreversible, given the minuscule levels of *free* zinc present in the body (*48*).

The clinical success of drugs that act through mechanism I (Figure 9) overshadows the therapeutic potential of chelators such as D-PEN that act by removing metal from the active site of metalloproteases (mechanism III in Figure 9). Efforts at drug design that search for tight-binding zinc protease inhibitors are biased against chelators acting according to mechanism I. To remove the catalytic zinc, mechanism III inhibitors must destabilize the environment surrounding the active-site metal. This weakens the instantaneous K_i and such a compound will escape notice if the appropriate mechanistic assays are not used.

Compared to the extensive research on inhibitors that bind tightly to metalloproteases, relatively little is known about the molecular mechanisms of how a chelator removes zinc from a metalloprotein. Although certain chelators such as OP have been known for two decades to catalyze zinc removal, their mechanisms of action have not been determined conclusively. Moreover, D-PEN is the first drug found to inhibit a zinc enzyme by catalytically removing the active-site zinc. Molecules showing weak inhibition in drug screens for tight-binding inhibitors might actually inhibit zinc proteases via a mechanism similar to D-PEN.

A reexamination of such inhibitors by the methodologies described in this paper could yield useful information on the determinants of a chelator mechanism. A new stopped-flow assay was used herein to study time-dependent inhibition. In this assay, enzyme and inhibitor are preincubated and mixed with substrate every 5−7 s, and the decrease in the initial velocity with time is used to detect inhibition (Figure 2). Inhibitors that catalyze metal removal are predicted to cause rapid inactivation of a zinc protease in the presence of a secondary chelator. Consequentially, this assay can be adapted to screen for such inhibitors by including a secondary chelator in the preincubation mixture. The use of the PAR assay for characterizing zinc removal can also be applied to extend our observations to other enzymes and inhibitors. Criteria learned from these studies could then be combined with methodologies used to design tight-binding inhibitors to improve chelators that act like D-PEN. For example, a substrate analogue could target D-PEN to specific enzymes, or the methyl groups could be altered to increase D-PEN's efficiency as a catalyst for zinc removal.

The ability of D-PEN to remove zinc from proteins may explain its side effects and contribute to its efficacy in the treatment of Wilson's disease. Of patients taking D-PEN for arthritis, 55−65% respond to the drug, but side effects limit the number of patients who benefit from the drug without complications to 41% (*3*). Many of the complications observed during D-PEN treatment, such as abnormalities in taste, skin disorders, and problems with wound healing, also appear in patients suffering from zinc deficiency (*6*, *49*). Nonspecific zinc removal by D-PEN could be overcome through rational drug design as discussed above. In Wilson's disease, however, this nonspecific zinc removal could benefit the patient by triggering endogenous chelators. Several studies demonstrate that D-PEN induces thionein expression (*50*−*53*). Thionein induction is thought to underlie the efficacy of zinc in treating Wilson's disease (*54*, *55*). It is surprising that a similar mechanism could underlie seemingly paradoxical treatments. While our proposals are not intended to refute the mechanism of D-PEN as a reductive chelator, these hypotheses may help to create a more complete

understanding of the mechanism of D-PEN in the treatment of Wilson's disease.

While various mechanisms have been proposed to explain the efficacy of D-PEN in its use to treat rheumatoid arthritis, none has been well characterized or generally accepted (*3*). Early research on the role of metalloproteases in arthritis suggested that the clinical efficacy of D-PEN may be related to its chelating ability (*56*, *57*). Because the metalloproteases used in those studies were components of crude extracts of human articular cartilage, a detailed mechanistic investigation of D-PEN inhibition was not undertaken (*57*). Given the emerging understanding of the role of MMPs in arthritis, it is interesting to speculate that the efficacy of D-PEN as a drug could be related to its ability to catalyze zinc release from metalloproteases. D-PEN has been reported to inhibit human gelatinase B, MMP-9, a suggested marker enzyme for rheumatoid arthritis (*58*). Preliminary experiments on the MMPs matrilysin and stromelysin show that D-PEN catalyzes zinc release from these enzymes (Chong and Auld, unpublished data). Further research is needed to determine the detailed mechanism of the inhibition of the MMPs and the physiological relevance of these results.

REFERENCES

1. Ondetti, M. A., Rubin, B., and Cushman, D. W. (1977) *Science 196*, 441−4.
2. Rasmussen, H. S., and McCann, P. P. (1997) *Pharmacol. Ther. 75*, 69−75.
3. Joyce, D. A. (1990) *Baillieres Clin. Rheumatol. 4*, 553−74.
4. Kean, W. F., Lock, C. J., and Howard-Lock, H. E. (1991) *Lancet 338*, 1565−8.
5. Peisach, J., and Blumberg, W. E. (1969) *Mol. Pharmacol. 5*, 200−9.
6. Munro, R., and Capell, H. A. (1997) *Br. J. Rheumatol. 36*, 104−9.
7. Conaghan, P. G., and Brooks, P. (1996) *Curr. Opin. Rheumatol. 8*, 176−82.
8. Chong, C. R., and Auld, D. S. (1998) *J. Trace Elem. Exp. Med. 11*, 335−336.
9. Bazzone, T. J., Sokolovsky, M., Cueni, L. B., and Vallee, B. L. (1979) *Biochemistry 18*, 4362−6.
10. Bicknell, R., Schaeffer, A., Auld, D. S., Riordan, J. F., Monnanni, R., and Bertini, I. (1985) *Biochem. Biophys. Res. Commun. 133*, 787−93.
11. Latt, S. A., Holmquist, B., and Vallee, B. L. (1969) *Biochem. Biophys. Res. Commun. 37*, 333−9.
12. Auld, D. S. (1988) *Methods Enzymol. 158*, 71−9.
13. Cha, J., Pedersen, M. V., and Auld, D. S. (1996) *Biochemistry 35*, 15831−8.
14. Simpson, R. T., Riordan, J. F., and Vallee, B. L. (1963) *Biochemistry 2*, 616−622.
15. Latt, S. A., Auld, D. S., and Vallee, B. L. (1972) *Anal. Biochem. 50*, 56−62.
16. Ng, M., and Auld, D. S. (1989) *Anal. Biochem. 183*, 50−6.
17. Holmquist, B. (1988) *Methods Enzymol. 158*, 6−12.
18. Auld, D. S. (1988) *Methods Enzymol. 158*, 13−4.
19. Tonomura, B., Nakatani, H., Ohnishi, M., Yamaguchi-Ito, J., and Hiromi, K. (1978) *Anal. Biochem. 84*, 370−83.
20. Latt, S. A., Auld, D. S., and Vallee, B. L. (1972) *Biochemistry 11*, 3015−22.
21. Morrison, J. F., and Walsh, C. T. (1988) *Adv. Enzymol. Relat. Areas Mol. Biol. 61*, 201−301.
22. Pollak, M., and Kuban, V. (1979) *Collect. Czech. Chem. Commun. 44*, 725−741.
23. Hunt, J. B., Neece, S. H., and Ginsburg, A. (1985) *Anal. Biochem. 146*, 150−7.
24. Latt, S. A., and Vallee, B. L. (1971) *Biochemistry 10*, 4263−70.
25. Banci, L., Bencini, A., Benelli, C., Gatteschi, D., and Zanchini, C. (1982) *Struct. Bonding 52*, 37−86.
26. Auld, D. S., and Vallee, B. L. (1987) in *Hydrolytic Enzymes* (Neuberger, H., and Brocklehurst, K., Eds.) pp 201−255, Elsevier, Amsterdam.
27. Holmquist, B., and Vallee, B. L. (1979) *Proc. Natl. Acad. Sci. U.S.A. 76*, 6216−20.
28. Bicknell, R., Schaffer, A., Bertini, I., Luchinat, C., Vallee, B. L., and Auld, D. S. (1988) *Biochemistry 27*, 1050−7.
29. Smith, E. L., and Hanson, H. T. (1949) *J. Biol. Chem. 175*, 803−813.
30. Sheikh, I. A., and Kaplan, A. P. (1987) *Arthritis Rheum. 30*, 138−45.
31. Auld, D. S. (1988) *Methods Enzymol. 158*, 110−4.
32. Auld, D. S. (1995) *Methods Enzymol. 248*, 228−42.
33. Harrington, P. C., and Wilkins, R. G. (1980) *J. Inorg. Biochem. 12*, 107−118.
34. Hirose, J., and Kidani, Y. (1981) *J. Inorg. Biochem. 14*, 313−26.
35. Rogers, R. J., and Billo, E. J. (1980) *J. Inorg. Biochem. 12*, 335−41.
36. Schwartz, M. A., Venkataraman, S., Ghaffari, M. A., Libby, A., Mookhtiar, K. A., Mallya, S. K., Birkedal-Hansen, H., and Van Wart, H. E. (1991) *Biochem. Biophys. Res. Commun. 176*, 173−9.
37. Geoghegan, K. F., Holmquist, B., Spilburg, C. A., and Vallee, B. L. (1983) *Biochemistry 22*, 1847−52.
38. Auld, D. S., Bertini, I., Donaire, A., Messori, L., and Moratal, J. M. (1992) *Biochemistry 31*, 3840−6.
39. Zhang, K., and Auld, D. S. (1995) *Biochemistry 34*, 16306−12.
40. Christianson, D. W., Mangani, S., Shoham, G., and Lipscomb, W. N. (1989) *J. Biol. Chem. 264*, 12849−53.
41. Johnson, W. H., Roberts, N. A., and Borkakoti, N. (1987) *J. Enzymol. Inhib. 2*, 1−22.
42. Brown, P. D., and Giavazzi, R. (1995) *Ann. Oncol. 6*, 967−74.
43. Garmer, D. R., Gresh, N., and Roques, B. P. (1998) *Proteins: Struct., Funct., Genet. 31*, 42−60.
44. De, B., Natchus, M. G., Cheng, M., Pikul, S., Almstead, N. G., Taiwo, Y. O., Snider, C. E., Chen, L., Barnett, B., Gu, F., and Dowty, M. (1999) *Ann. N.Y. Acad. Sci. 878*, 40−60.
45. Kiefer, L. L., Paterno, S. A., and Fierke, C. A. (1995) *J. Am. Chem. Soc. 117*, 6831−6837.
46. Lesburg, C. A., and Christianson, D. W. (1995) *J. Am. Chem. Soc. 117*, 6838−6844.
47. Christianson, D. W., and Fierke, C. A. (1996) *Acc. Chem. Res. 29*, 331−39.
48. Canzoniero, L. M., Turetsky, D. M., and Choi, D. W. (1999) *J. Neurosci. 19*, RC31 (1−6).
49. Prasad, A. S. (1985) *Annu. Rev. Nutr. 5*, 341−63.
50. Goering, P. L., Tandon, S. K., and Klaassen, C. D. (1985) *Toxicol. Appl. Pharmacol. 80*, 467−72.
51. Heilmaier, H. E., and Summer, K. H. (1985) *Arch. Toxicol. 56*, 247−51.
52. Mullin, C. H., Abel, J., Klein, D., and Summer, K. H. (1988) *J. Trace Elem. Electrolytes Health Dis. 2*, 43−7.
53. Yuzbasiyan-Gurkan, V., Grider, A., Nostrant, T., Cousins, R. J., and Brewer, G. J. (1992) *J. Lab. Clin. Med. 120*, 380−6.
54. Brewer, G. J., Hill, G. M., Dick, R. D., Nostrant, T. T., Sams, J. S., Wells, J. J., and Prasad, A. S. (1987) *J. Lab. Clin. Med. 109*, 526−31.
55. Brewer, G. J., and Yuzbasiyan-Gurkan, V. (1992) *Medicine (Baltimore) 71*, 139−64.
56. Crawhall, J. C., Lecavalier, D., and Ryan, P. (1979) *Biopharm. Drug Dispos. 1*, 73−95.
57. Sapolsky, A. I., Keiser, H., Howell, D. S., and Woessner, J. F., Jr. (1976) *J. Clin. Invest. 58*, 1030−41.
58. Norga, K., Grillet, B., Masure, S., Paemen, L., and Opdenakker, G. (1996) *Clin. Rheumatol. 15*, 31−4.

BI000101+